Spatiotemporal Analysis of Copper Homeostasis in *Populus trichocarpa* Reveals an Integrated Molecular Remodeling for a Preferential Allocation of Copper to Plastocyanin in the Chloroplasts of Developing Leaves[1][C][W][OA]

Karl Ravet, Forest L. Danford[2], Alysha Dihle, Marco Pittarello[3], and Marinus Pilon*

Biology Department, Colorado State University, Fort Collins, Colorado 80523

Plastocyanin, which requires copper (Cu) as a cofactor, is an electron carrier in the thylakoid lumen and essential for photoautotrophic growth of plants. The Cu microRNAs, which are expressed during Cu deprivation, down-regulate several transcripts that encode for Cu proteins. Since plastocyanin is not targeted by the Cu microRNAs, a cofactor economy model has been proposed in which plants prioritize Cu for use in photosynthetic electron transport. However, defects in photosynthesis are classic symptoms of Cu deprivation, and priorities in Cu cofactor delivery have not been determined experimentally. Using hydroponically grown *Populus trichocarpa* (clone Nisqually-1), we have established a physiological and molecular baseline for the response to Cu deficiency. An integrated analysis showed that Cu depletion strongly reduces the activity of several Cu proteins including plastocyanin, and consequently, photosynthesis and growth are decreased. Whereas plastocyanin mRNA levels were only mildly affected by Cu depletion, this treatment strongly affected the expression of other Cu proteins via Cu microRNA-mediated transcript down-regulation. Polyphenol oxidase was newly identified as Cu regulated and targeted by a novel Cu microRNA, *miR1444*. Importantly, a spatiotemporal analysis after Cu resupply to previously depleted plants revealed that this micronutrient is preferentially allocated to developing photosynthetic tissues. Plastocyanin and photosynthetic electron transport efficiency were the first to recover after Cu addition, whereas recovery of the other Cu-dependent activities was delayed. Our findings lend new support to the hypothesis that the Cu microRNAs serve to mediate a prioritization of Cu cofactor use. These studies also highlight poplar as an alternative sequenced model for spatiotemporal analyses of nutritional homeostasis.

Photosynthetically active tissues have a high demand for the redox active metal ions copper (Cu), iron (Fe), and manganese (Mn), which are used as cofactors in photosynthetic electron transport (Raven et al., 1999). In plant chloroplasts, three major Cu proteins occur. Plastocyanin (PC) is a blue Cu protein of the thylakoid lumen that is absolutely required for photosynthetic electron transport in plants (Weigel et al., 2003). Polyphenol oxidase (PPO) is a binuclear Cu protein in the thylakoid lumen that catalyzes (1) the *o*-hydroxylation of monophenols to *o*-diphenols and (2) the oxidation of the latter to produce *o*-quinones (Mayer, 2006). PPO is found in several plants (Mayer, 2006), but it is not found in Arabidopsis (*Arabidopsis thaliana*; Schubert et al., 2002). Copper/zinc superoxide dismutase (Cu/ZnSOD) is a major Cu protein in the stroma and cytosol (for review, see Pilon et al., 2011). Cu is also important for cytochrome *c* oxidase (COX), the terminal oxidase in the mitochondria, which requires three Cu atoms per enzyme (Carr and Winge, 2003), and for the ethylene receptors (Rodríguez et al., 1999). Other Cu proteins for which the biological function is not fully clear include the apoplastic proteins plantacyanin, members of the multicopper oxidase laccase family, ascorbate oxidase, and amine oxidase (for review, see Cohu and Pilon, 2010).

The system for Cu uptake and intracellular delivery has been described in some detail (for review, see Burkhead et al., 2009; Puig and Peñarrubia, 2009). Cu enters the cytoplasm via members of the COPT (for Cu transporter) family (Kampfenkel et al., 1995; Sancenón et al., 2003, 2004; Andrés-Colás et al., 2010; Garcia-Molina et al., 2011). In the cytosol, three Cu

chaperones have been described. The antioxidant 1 (ATX) protein and the Cu chaperone (CCH) interact with the P-type ATPase transporters HMA5 and HMA7 (HMA for heavy metal-associated domain superfamily; Andrés-Colás et al., 2006; Puig et al., 2007). HMA5 is important for Cu export from the cell and may be a control point for root-shoot translocation (Andrés-Colás et al., 2006). HMA7 (also called RAN1 for responsive to antagonist 1) is required to bring Cu to the ethylene receptors in an early endomembrane system compartment (Hirayama et al., 1999). The Cu chaperone for SOD (CCS) is found both in the cytosol and the chloroplast, where it is required for Cu/ZnSOD maturation (Chu et al., 2005). The P-type ATPase of Arabidopsis PAA1 (HMA6) in the chloroplast envelope serves to transport Cu to the chloroplast and therefore is required for optimal activation of chloroplastic Cu/ZnSOD and PC (Tabata et al., 1997; Shikanai et al., 2003). The P-type ATPase transporter PAA2 (HMA8) of the thylakoids functions in Cu delivery to the lumen and therefore affects PC activity (Abdel-Ghany et al., 2005; Bernal et al., 2007). It is not known how Cu enters the mitochondria, but the assembly system for COX, including several Cu chaperones in the mitochondrion, seems to be essentially conserved from yeast to plants (for review, see Burkhead et al., 2009).

The conserved transcription factor SPL7 (for squamosa promoter binding protein-like 7) regulates Cu homeostasis in Arabidopsis, where it mediates two major responses when Cu is limited (Yamasaki et al., 2009). SPL7 is required for the up-regulation of cellular Cu uptake and assimilation mechanisms, which is highlighted by the up-regulation of the expression of the plasma membrane COPT1 Cu transporter (Yamasaki et al., 2009). On low Cu, SPL7 also is required for expression of the so-called Cu microRNAs (miRNAs; Burkhead et al., 2009), which in turn down-regulate transcripts for the Cu proteins CCS, Cu/ZnSOD1 (CSD1), and CSD2 (targets of *miR398*), plantacyanin (target of *miR408*), and several laccases (targets of *miR397*, *miR408*, and *miR857*; Sunkar et al., 2006; Yamasaki et al., 2007; Abdel-Ghany and Pilon, 2008; Dugas and Bartel, 2008; Cohu et al., 2009; Yamasaki et al., 2009). A Cu economy model has been hypothesized in which the miRNA-mediated mechanism saves Cu for the most essential Cu proteins, such as COX and PC, during impending deficiency (Burkhead et al., 2009, and refs. therein). However, direct evidence for the idea that PC and COX might be priorities for Cu delivery has to this point been lacking.

Classic symptoms of Cu deficiency include reduction in biomass, chlorosis, lack of photosynthetic activity, rolling of leaves and defects in plant morphology, delay in flowering, and desiccation (Marschner, 1995). The strong effect of Cu deficiency on photosynthesis might suggest that PC is not at all a prime target for Cu delivery. However, a detailed description of Cu deficiency that integrates both physiological data and effects at the molecular level is lacking. Cu has been classified as an immobile element because, unlike what is found for nitrogen, plants do not efficiently reallocate Cu from source leaves to developing sink tissue (Marschner, 1995). Partitioning of Cu, Fe, and Zn has been followed over the life span of Arabidopsis, revealing some ecotype-specific differences in uptake and allocation (Waters and Grusak, 2008). These studies also revealed relations between organs and the capacity to redistribute Cu, Fe, and Zn during senescence and the possible roles of two yellow stripe-like transporters (YSL1 and YSL3) in the redistribution of these three metals to developing fruit tissue. The above-mentioned miRNA-mediated Cu economy model, however, has been difficult to test in Arabidopsis, due to its small size and the difficulty of inducing Cu deficiency in photosynthetically growing Arabidopsis seedlings without causing strong secondary effects (Abdel-Ghany and Pilon, 2008; Abdel-Ghany, 2009).

With its size and fast growth, poplar (*Populus trichocarpa*; clone Nisqually-1) would be an excellent model to study spatial and temporal effects of Cu depletion and resupply. Because of the availability of a sequenced genome (Tuskan et al., 2006), physiological studies can now be integrated with molecular analyses in poplar. The aim of this study was to analyze the effects of moderate Cu deficiency in poplar and to characterize the physiological and molecular responses to Cu depletion and resupply with emphasis on chloroplast functions. Poplar proved to be an excellent model for detailed spatiotemporal analysis of the dynamics of Cu homeostasis and for integrating physiological and molecular level studies. The results obtained lend new and very strong support to the Cu economy model, where energy-related electron transport functions, especially in developing leaves, receive priority in Cu delivery over other major Cu enzymes. In addition, PPO was identified as a Cu-regulated protein that is targeted by a novel Cu miRNA.

RESULTS

Effects of Cu Depletion on Growth and Photosynthetic Functions

Cuttings taken from soil-grown poplar plants contained Cu at 12.8 ± 5.9 μg g^{-1} dry weight. After rooting, these cuttings were grown in hydroponics (Fig. 1A) on one-tenth-strength modified Hoagland solution (Hoagland and Arnon, 1950; Epstein and Bloom, 2005), which contains 50 nM $CuSO_4$, a concentration shown to be sufficient for a range of plants (Cohu and Pilon, 2007). To deplete Cu, we omitted it from the salt solution (deficiency condition). The cuttings grown without added Cu showed no deficiency symptoms for the first 2.5 weeks, which we ascribe to the Cu content of the cuttings. The first symptoms of deficiency became apparent after 2.5 weeks, when growth started to slow down; growth eventually ceased after 4 weeks (Fig. 1B). The symptoms of Cu
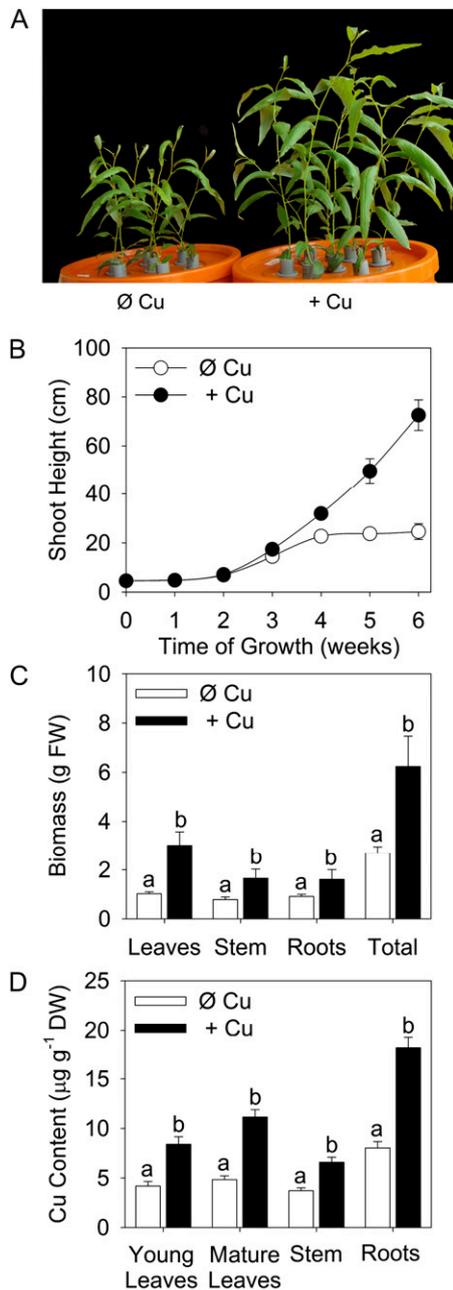
Figure 1. Cu deficiency reduces poplar growth. Poplar cuttings were grown hydroponically in the presence of 50 nM CuSO$_4$ (+ Cu) or without added Cu (Ø Cu). A, Five-week-old plants. B, Growth curve of poplar during 6 weeks. Growth was monitored by measurement of shoot height. Values are given as averages ± SD ($n = 15$). C, Fresh weights (FW) produced after 5 weeks of growth. Values are given as averages ± SD ($n = 10$). D, Cu content (μg g^{-1} dry weight [DW]) was measured by ICP-AES. Values are given as averages ± SD ($n = 6$). Different letters above bars in C and D represent significant differences ($P < 0.05$) within organs.

deficiency were largely reversible if Cu was added before week 6 (see below). However, tissue of deficient plants started to die off after 7 weeks, at which time secondary effects started to dominate. In contrast,

poplar plants grown on 50 nM Cu (sufficient condition) kept growing vigorously for over 6 weeks (Fig. 1B), at which time the space below growth lights started to be limiting. Nevertheless, these plants remained vigorous for at least 3 months, reaching heights of 150 cm (data not shown). In order to avoid unspecific secondary effects, we compared the physiology and biochemistry of 5-week-old sufficient and deficient plants.

After 5 weeks, a dramatic difference in growth was apparent between the 50 nM Cu and no-Cu treatments (Fig. 1). Deficient plants showed stunted growth, as evidenced by a large reduction in plant height (Fig. 1, A and B) and a reduction in the biomass of roots, stems, and especially leaves (Fig. 1C). The Cu content was drastically reduced in all plant parts of deficient plants and had dropped to below 5 μg g^{-1} dry weight in both young and old leaves and stems (Fig. 1D), values that are considered below the typical critical deficiency level for most plants (Marschner, 1995). The elemental composition for Fe, nickel, magnesium, and carbon was not affected by Cu treatment (Supplemental Table S1). However, we did observe significantly higher levels of Mn in both leaves and stems for Cu-deficient plants. Zn levels were also elevated in deficient plants, but only in the leaves (Supplemental Table S1). We did not observe changes for other elements, including molybdenum and phosphorus, which are not mentioned in Supplemental Table S1.

Developing leaves of deficient plants were slightly chlorotic and had a 27% reduction in chlorophyll content when compared with the Cu-sufficient ones (Fig. 2A). To evaluate the effects of Cu deficiency on the photosynthetic electron transport efficiency, we analyzed the chlorophyll fluorescence parameters electron transport rate (ETR), nonphotochemical quenching (NPQ), and maximum quantum efficiency of the PSII (F_v/F_m; Maxwell and Johnson, 2000). The relative ETR was estimated as a function of light intensity (Fig. 2B). In young and mature leaves, Cu deficiency affected ETR very dramatically, and the same low level of ETR was observed in the depleted plants for both types of leaves. However, the mature leaves of sufficient plants also showed reduction in ETR (Fig. 2B) compared with young leaves of the same plants, despite the higher Cu content of these older leaves (Fig. 1D). The parameter NPQ mainly estimates heat dissipation of excess light capture by PSII and depends on acidification of the thylakoid lumen, which in turn depends on electron transport efficiency (Müller et al., 2001). NPQ was drastically affected by Cu deficiency in young leaves, whereas this parameter was much less affected by deficiency in mature leaves (Fig. 2C). The parameter F_v/F_m for dark-adapted plants is indicative of the efficiency of PSII and used as an indication of photo-inhibition caused by stress imposed on PSII. Cu depletion did not affect F_v/F_m in mature leaves, whereas a small but significant effect on F_v/F_m was seen in young leaves (Fig. 2D). In summary, electron transport capacity was strongly affected by Cu depletion, especially in developing leaves.

Table I. *Cu-related proteins in poplar*

Poplar sequences were retrieved from the NCBI. Locus (POPTRDRAFT), protein (XP), and gene (XM) accession numbers are given for PC, CSD, CCS, and PPO. n.a., Not available.

Locus Name	Locus Accession No.	Protein Accession No.	Gene Accession No.
PCa	POPTRDRAFT_652151	XP_002307754.1	XM_002307718.1
PCb	POPTRDRAFT_813630	XP_002300679.1	XM_002300643.1
CCS	POPTRDRAFT_674097	XP_002331793.1	XM_002331757.1
CSD1a	POPTRDRAFT_568791	XP_002316852.1	XM_002316816.1
CSD1b	POPTRDRAFT_786663	XP_002331714.1	XM_002331678.1
CSD2a	POPTRDRAFT_568257	XP_002316632.1	XM_002316596.1
CSD2b	POPTRDRAFT_585475	XP_002331712.1	XM_002331676.1
PPO1	POPTRDRAFT_568791	XP_002316852.1	XM_002316816.1
PPO2	POPTRDRAFT_786663	XP_002331714.1	XM_002331678.1
PPO3	POPTRDRAFT_568257	XP_002316632.1	XM_002316596.1
PPO4	POPTRDRAFT_585475	XP_002331712.1	XM_002331676.1
PPO5	POPTRDRAFT_674097	XP_002331793.1	XM_002331757.1
PPO6	POPTRDRAFT_790794	XP_002336111.1	XM_002336072.1
PPO7	POPTRDRAFT_275813	n.a.	n.a.
PPO8	POPTRDRAFT_235525	n.a.	n.a.
PPO9	POPTRDRAFT_1118063	XP_002331795.1	XM_002331759.1
PPO10	POPTRDRAFT_800778	XP_002306113.1	XM_002306077.1
PPO11	POPTRDRAFT_794816	XP_002338396.1	XM_002338356.1
PPO12	POPTRDRAFT_276236	XP_002331796.1	XM_002331760.1
PPOp	POPTRDRAFT_275837	n.a.	n.a.

Cu Depletion Affects the Function of Major Cu Proteins in the Chloroplast and Cytosol

PC is a major Cu protein in green tissues with a pivotal role in photosynthetic electron transport (Burkhead et al., 2009). The poplar genome (Tuskan et al., 2006) encodes for two PC isoforms with a predicted mass of 10.5 kD for the mature proteins. The antiserum raised against spinach (*Spinacia oleracea*) PC (Abdel-Ghany et al., 2005) detected protein bands at 14 and 6 kD on immunoblots of poplar samples (Fig. 3A). However, only the lower band at 6 kD was detected in isolated chloroplasts and thylakoids, and proteomic analysis via mass spectroscopy identified this band as a mixture of PCa and PCb, while the upper band is unrelated (data not shown). We analyzed the effect of Cu depletion on PC content by immunoblotting (Fig. 3A). The protein cytosolic Fru-1,6-bisphosphatase (cFBPase) was used as a loading control. In Cu-sufficient plants, PC was detected in green tissues, especially in the leaves, but it was absent in roots. Interestingly, the PC content of leaves was severely affected by Cu depletion, especially in the young leaves. Quantification showed that the PC content decreased to the detection limit in young leaves and to about 15% in mature leaves by depletion of Cu. Thus, the reduction in PC content largely explains the strong effect of Cu depletion on electron transport. We analyzed PC transcript levels to investigate if the depletion of PC could be explained by an effect of Cu on the mRNA accumulation of both PC isoforms (Fig. 3B). In Arabidopsis, PC mRNA levels do not respond to Cu limitation, whereas the abundance of the polypeptide of the major isoform PC2 was affected (Abdel-Ghany and Pilon 2008; Abdel-Ghany

2009). It was surprising, therefore, that the abundance of both poplar PC transcripts was slightly decreased by Cu depletion in young leaves, where an approximately 25% reduction was observed (Fig. 3B). However, the extent of the changes in PC transcript levels could not fully account for the much lower accumulation of PC protein on low Cu. Therefore, reduced stability in the absence of the Cu cofactor is probably responsible for most of the drastic effect of Cu on PC protein accumulation.

It has been proposed that plants under deficiency save Cu for PC by down-regulating other Cu proteins, including the Cu/ZnSODs and their metallochaperone CCS (Burkhead et al., 2009). Phylogenetic analysis revealed that the poplar genome encodes two isoforms closely related to the Arabidopsis cytosolic Cu/ZnSOD AtCSD1 and two isoforms closely related to AtCSD2, the chloroplastic counterpart (Supplemental Fig. S1). Fractionation experiments indicated that the Cu/ZnSOD band with the highest mobility on native activity gels (Fig. 4A) corresponds to the chloroplast-localized CSD2s, whereas the bands with lower mobility are not recovered in isolated chloroplasts (data not shown). In accordance, the antibody raised against the Arabidopsis chloroplastic AtCSD2 recognized two bands (Fig. 4B), which were both found in the chloroplast stroma after fractionation (data not shown). The CSD1 antibody recognized two isoforms in poplar (Fig. 4B), which were not found in plastids (data not shown). The activity and protein accumulation of all cytosolic CSD1 and plastidic CSD2 isoforms was severely affected by Cu depletion (Fig. 4, A and B). Interestingly, the effect of Cu on Cu/ZnSOD activity and accumulation was most pronounced in the young leaves (Fig. 4, A and B). The loss of Cu/ZnSOD
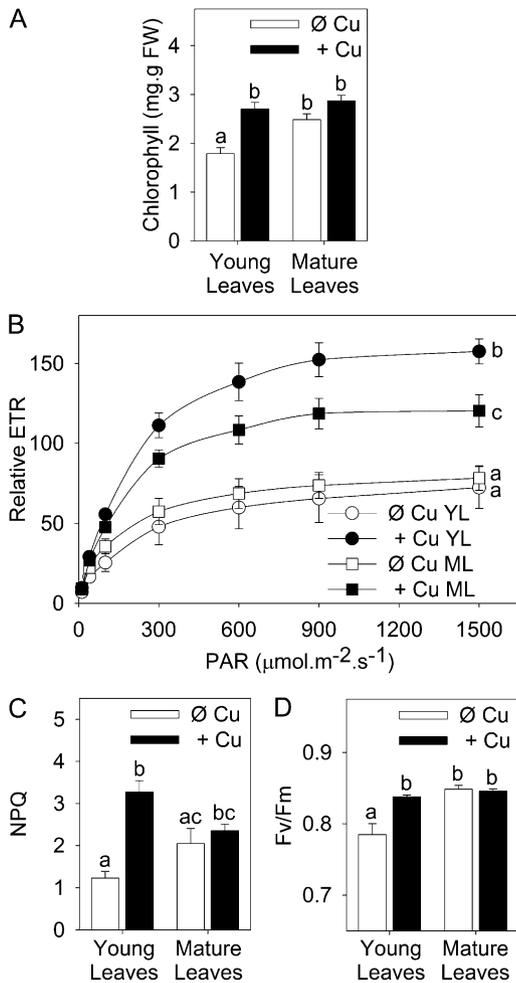
Figure 2. Cu deficiency alters photosynthetic performance. A, Leaf chlorophyll content. Values are given as averages ± sd ($n = 15$). FW, Fresh weight. B, Response curve of the relative ETR to light intensities ranging from 40 to 1,500 μmol m^{-2} s^{-1} in young leaves (YL) and mature leaves (ML). Values are given as averages ± sd ($n = 6$). C, NPQ measured at 600 μmol m^{-2} s^{-1}. Values are given as averages ± sd ($n = 6$). D, F_v/F_m of dark-adapted plants. Values are given as averages ± sd ($n = 6$). Different letters above bars (in A, C, and D) or points (in B) represent significant differences between groups ($P < 0.05$).

isoforms in Cu-deficient leaves was fully explained by a decrease in mRNA levels of all *CSD1* and *CSD2* isoforms (Fig. 4C). A decrease in *CCS* transcript accumulation was also observed (Supplemental Fig. S1). Interestingly, all these transcripts exhibit potential *miR398* target sites (Supplemental Fig. S1). In poplar, the region of 500 bp upstream of the *miR398* precursor stem loop for *miR398b* and *miR398c* contains eight and 10 *GTAC* elements, respectively (Supplemental Fig. S2), motifs described as potential Cu-responsive elements in *Chlamydomonas* (Kropat et al., 2005) and in Arabidopsis (Yamasaki et al., 2009). Indeed, *miR398b* and *miR398c* accumulation was induced by Cu deficiency in both young and mature deficient leaves (Fig. 4D). Surprisingly, *miR398a* was also induced, but only

in old leaves (Fig. 4D), despite the presence of only one *GTAC* motif in its promoter region (Supplemental Fig. S2).

To investigate if other major Cu proteins are regulated by Cu availability in poplar, we undertook a proteomic approach. Coomassie Brilliant Blue staining after SDS-PAGE separation of total protein samples indicated that an abundant protein of about 68 kD accumulates in leaves only in Cu-sufficient plants (Fig. 5A). This band was excised from the gel and analyzed by mass spectroscopy after trypsin digestion. Among the different proteins found in the sample (Supplemental Fig. S3), the most abundant and most strongly Cu-regulated protein was identified as a novel protein closely related to PPO. Therefore, we analyzed the effect of Cu depletion on PPO activity in poplar tissues. Activity assays indicated that PPO activity is present in all tissues and that it strongly depends on Cu nutrition (Fig. 5B). Tropolone, a Cu chelator acting as a specific PPO inhibitor (Kahn and Andrawis, 1985; Valero et al., 1991), completely blocked activity (Fig. 5B), showing the specificity of the assay and the strict dependence on Cu for PPO enzymatic activity. Fractionation experiments indicated that high PPO activity was recovered in the thylakoid lumen fraction of isolated chloroplasts (data not shown). Native gel assays indicated that multiple isoforms of PPO are affected by Cu (Fig. 5B, bottom panel). PPO has been
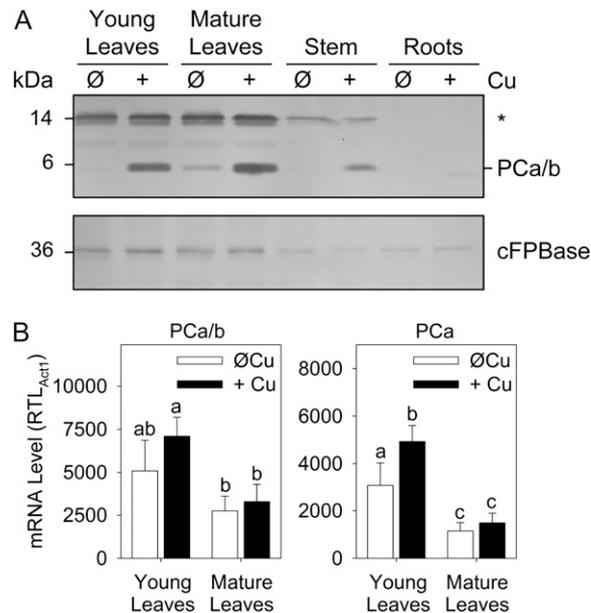

Figure 3. Cu deficiency reduces PC abundance in poplar. A, Immunodetection of PC (PCa/b). Total soluble proteins (20 μg) were fractionated by SDS-PAGE (15% gel) and blotted onto membranes. The asterisk indicates nonspecific cross-reactivity of the PC antibody. cFBPase was used as a loading control. B, Total PC (PCa/b) and PCa relative transcript levels (RTL) were determined using qRT-PCR. Values are normalized relative to Actin1 expression and given as averages ± sd ($n = 3$). Different letters above bars represent significant differences ($P < 0.05$).

shown to be induced by wounding (Constabel et al., 2000). Thus, we investigated the effect of Cu feeding on the induction of PPO activity following wounding (Fig. 5C). Strikingly, Cu was found to be required for a proper induction of PPO.
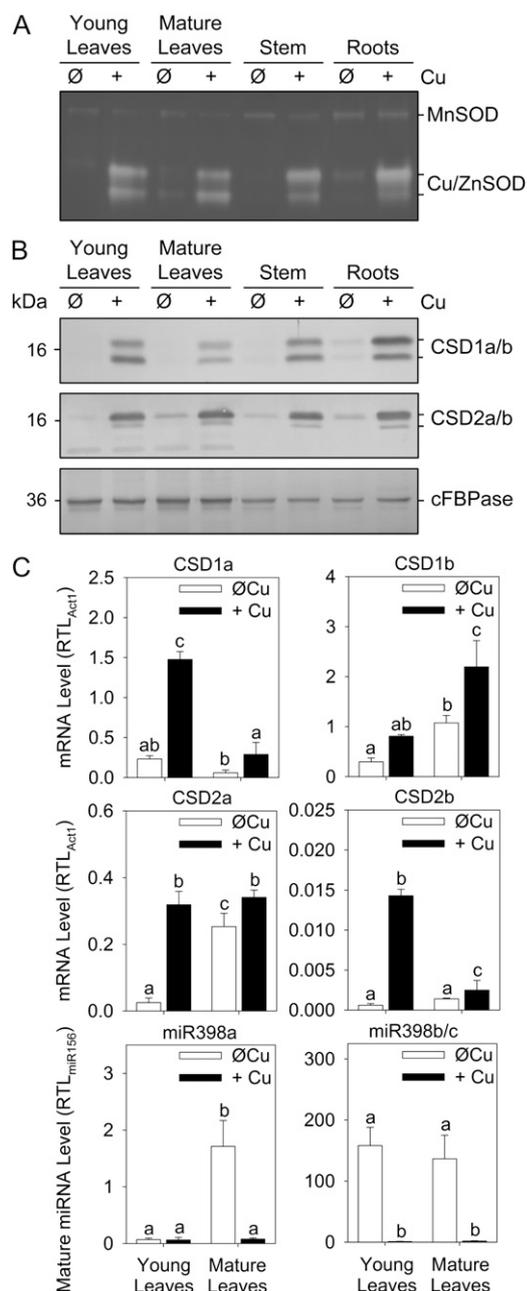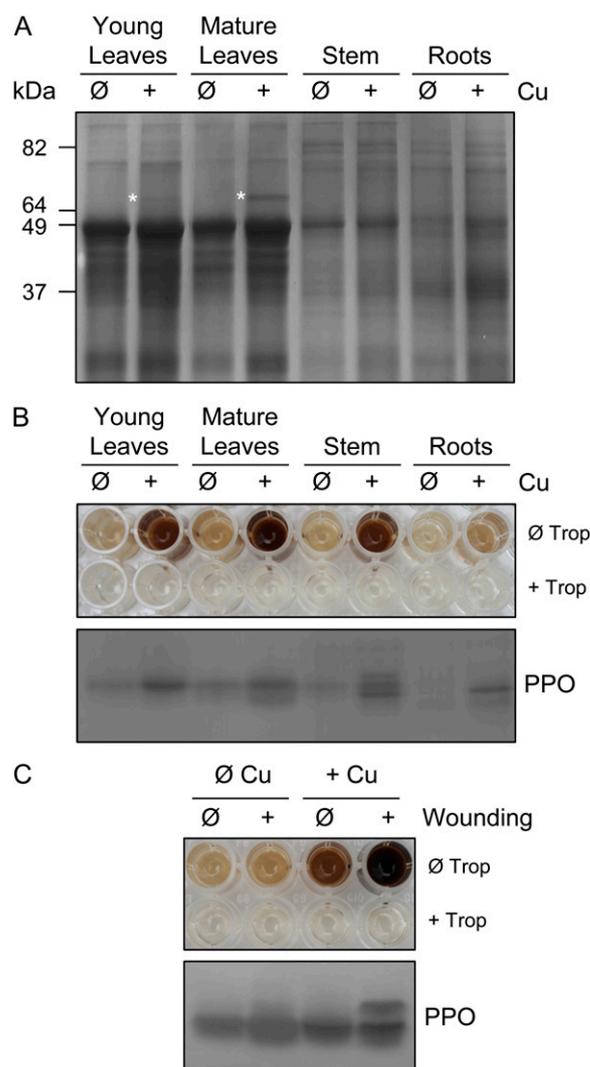

Figure 4. *miR398* regulates the Cu/ZnSODs CSD1 and CSD2 in response to Cu deficiency. A, Total soluble proteins (40 μg) were fractionated on a nondenaturing 15% acrylamide gel and stained for total SOD activity. B, Immunodetection of the cytosolic (CSD1a/b) and plastidial (CSD2a/b) Cu/ZnSOD isoforms. cFBPase was used as a loading control. Total soluble proteins (20 μg) were fractionated by SDS-PAGE (15% gel) and blotted. C, RNA expression levels. CSD1a/b and CSD2a/b relative transcripts levels (RTL) were determined using qRT-PCR. Values are normalized relative to Actin1 expression and are given as averages $\pm$ SD ($n = 3$). Mature *miR398a* and *miR398b/c* relative transcripts levels were determined using qRT-PCR. Values are normalized relative to *miR156* expression and are given as averages $\pm$ SD ($n = 3$). Different letters above bars represent significant differences ($P < 0.05$) between groups.

Figure 5. Identification of the PPOs as Cu-regulated proteins in poplar. A, Total soluble protein profile of Cu-sufficient and Cu-deficient poplar. Total soluble proteins (20 μg) were fractionated by SDS-PAGE (15% gel) and stained by Coomassie Brilliant Blue. Stars indicate the approximately 68-kD Cu-regulated protein subjected to liquid chromatography-mass spectrometry identification. B, Effects of Cu deficiency on PPO activity. For the browning assay (top panel), 400 μg of total soluble protein was incubated at room temperature for 36 h (Ø Trop). For control samples, a PPO-specific inhibitor, tropolone, was added at 400 μM (+ Trop). For the in-gel PPO activity assay (bottom panel), 40 μg of native protein was fractionated by SDS-PAGE (10% gel) and stained for PPO activity using the L-3,4-dihydroxy-Phe method. C, Effect of Cu deficiency on the induction of PPO activity in response to wounding. Poplar cuttings were mechanically wounded, and total leaves were sampled after 48 h. Experiments were conducted as described in B. [See online article for color version of this figure.]

Several PPO sequences had been annotated in the poplar genome. After amino acid sequence alignments and phylogenetic analysis of all available PPO-like sequences (Fig. 6A; Supplemental Fig. S4), we called the newly identified protein PPO12. The genomic *PPO12* sequence encodes a precursor with a predicted bipartite N-terminal targeting signal consisting of a chloroplast transit sequence and a thylakoid signal sequence with a twin Arg motif. Therefore, PPO12 is
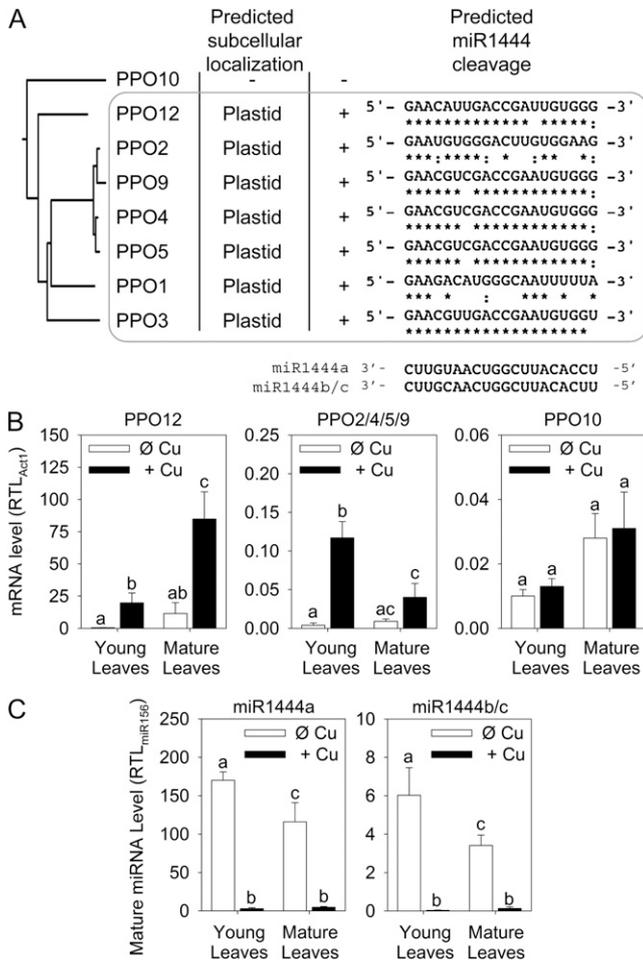

predicted to be active in the thylakoid lumen (Supplemental Fig. S4). Consistently, peptides were detected for almost the entire mature sequence in the proteomic analysis but none for the cleaved targeting signal (Supplemental Fig. S3). The phylogenetic analysis also reveals that all PPO sequences except the one of PPO10 are predicted to be chloroplast lumen located and to group together (Fig. 6A; Supplemental Fig. S4). PPO10, the related sequence without targeting information, forms an outgroup (Fig. 6A; Supplemental Fig. S4).

Transcript levels of the putative plastid isoforms *PPO12*, *PPO2/4/5/9* (detected by one primer pair; see "Materials and Methods"; Fig. 6B), and *PPO1/3* (data not shown) are regulated by Cu, while the one of PPO10 is not (Fig. 6B). Interestingly, all putative chloroplastic *PPO* sequences are predicted targets of a miRNA, *miR1444* (Fig. 6A; Supplemental Fig. S4). *miR1444* was previously shown to target PPO2 in poplar (Lu et al., 2008). There are three loci for miR1444 in poplar, but this miRNA is absent from Arabidopsis, which also does not express any PPO (Schubert et al., 2002). Since PPO is a Cu enzyme, we considered that *miR1444* could be a member of the Cu miRNAs. The region of 500 bp upstream of the stem loop for all three *miR1444* loci is enriched with five to six *GTAC* putative Cu-regulatory elements (Supplemental Fig. S2). Indeed, *miR1444* expression was strongly up-regulated in leaves of plants grown under Cu deprivation (Fig. 6C). *miR1444*, therefore, is a new member of the Cu miRNAs that down-regulates the chloroplastic PPOs under Cu deprivation in poplar.

Cu is also an important cofactor of mitochondrial COX and required for its stability and accumulation (Carr and Winge, 2003). The COXII subunit of COX is a highly conserved and mitochondrially encoded Cu-binding subunit of 29 kD. Remarkably, immunoblotting using COXII-specific antiserum indicated that COXII levels were not significantly affected by Cu in our experimental conditions (Supplemental Fig. S5).

Figure 6. *miR1444* is a novel Cu miRNA that down-regulates the plastid-targeted PPOs in poplar. A, Phylogenic analysis of the PPO family in the poplar genome. The analysis is based on the full-length coding sequences available on NCBI, and the tree was built using ClustalW. The subcellular location predictions were performed using TargetP. The *miR1444* target sites in PPO genes were searched using the miRBase database. Watson-Crick pairings (asterisks) and G/U wobble pairings (colons) with at least one of the *miR1444s* are indicated. B, PPO12, PPO2/4/5/9, and PPO10 relative transcript levels (RTL) were determined using qRT-PCR. PPO2, -4, -5, and -9 are highly similar, and a primer pair was used that detects all four of these isoforms. Values are normalized relative to Actin1 expression and are given as averages ± SD (n = 3). C, *miR1444a* and *miR1444b/c* relative transcript levels were determined using qRT-PCR. Values are normalized relative to *miR156* expression and are given as averages ± SD (n = 3). Different letters above bars represent significant differences (P < 0.05) between groups.

PC in Young Leaves Is a Preferred Target for Cu Delivery during Recovery from Depletion

We had hypothesized that PC would be a preferred target for Cu delivery during impending deficiency (Burkhead et al., 2009). This idea was based on the observed Cu miRNA-mediated down-regulation of several Cu proteins in Arabidopsis (Abdel-Ghany et al., 2005; Yamasaki et al., 2007; Abdel-Ghany and Pilon 2008; Dugas and Bartel, 2008; Cohu et al., 2009) as well as in *Brassica* species, tomato (*Solanum lycopersicum*), maize (*Zea mays*), and rice (*Oryza sativa*; Cohu and Pilon, 2007). However, in Arabidopsis, PC2 protein was reported to be strongly affected by Cu (Abdel-Ghany 2009), and PC protein levels were also affected by Cu in poplar (Fig. 3) with a simultaneous loss of photosynthetic electron transport function (Fig. 2). These observations seem to challenge the idea that Cu is preferentially allocated to PC. We reasoned,

however, that micronutrient allocation is a dynamic process and that a spatiotemporal analysis would be required to gain insight into the priorities of Cu delivery to biochemical targets.

To investigate which Cu proteins are prioritized for Cu delivery during a recovery from Cu deficiency, we analyzed the recovery of Cu-dependent enzymes and processes in different organs over time. Plants that had been depleted of Cu for 5 weeks were given 50 nM CuSO$_4$, and the recovery of Cu proteins and enzyme activity were assayed over 5 d. Representative protein data for leaves are given in Figure 7, and a quantification of three separate experiments is shown in Figure 8 together with Cu levels and activity measurements. Strikingly, immunoblot analysis and quantification indicate that PC levels recovered quickly in young leaves and not as fast in mature leaves. After 2 d, both PC and Cu levels started to rise in young leaves (Figs. 7A and 8, A and B). In older leaves, PC and Cu came up after 5 d only (Figs. 7B and 8, A and C). The recovery of PC protein in young leaves and in older leaves reflects the recovery of Cu levels in these organs.
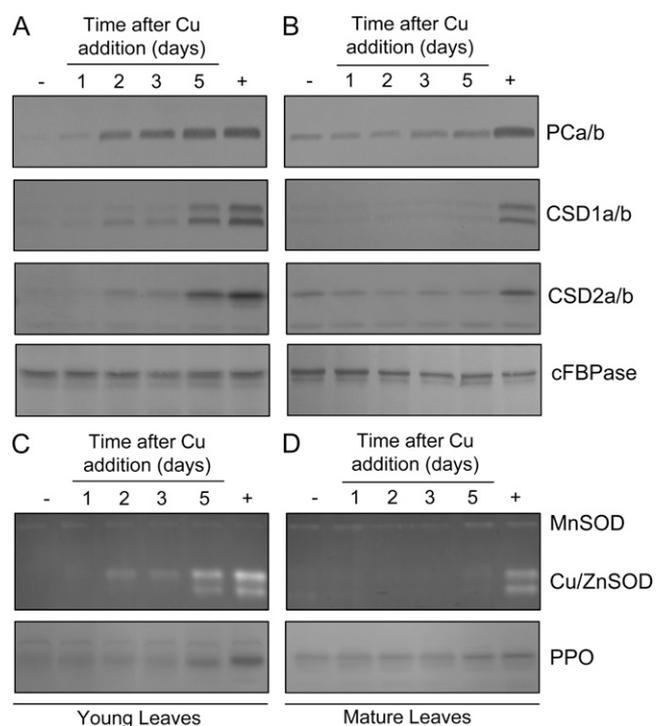
In contrast to what was observed for PC, Cu/ZnSOD protein levels showed a much-delayed recovery even in the young leaves (Figs. 7 and 8, B and C).

The fast rise in PC levels was also reflected in the very quick recovery of PC-dependent electron transport activity, especially in developing leaves (Fig. 8, D and E). In contrast, the activities of Cu/ZnSOD and PPO were delayed by about 2 d relative to ETR activity in the young leaves (Figs. 7, C and D, and 8, D and E). The recovery of Cu/ZnSOD and PPO activity was even slower in the older leaves. The recovery of PC, Cu/ZnSOD, and PPO in stems mirrored that in old leaves (Supplemental Fig. S6). Surprisingly, the recovery of Cu/ZnSOD in roots was even further delayed compared with green tissue (Supplemental Fig. S6). Together, these data clearly indicate that young leaves are preferential organs for Cu delivery when Cu is added back after starvation. Furthermore, at the molecular level, PC is the preferred target protein for Cu resupply.

DISCUSSION

It has been hypothesized, based on observations in Arabidopsis, that plants save Cu for the most essential Cu proteins, such as COX and PC, during impending Cu deficiency. This Cu economy model, however, has been difficult to test in Arabidopsis. Poplar turned out to be an excellent and very reproducible model to gain insight into the spatial and temporal effects of Cu depletion and resupply. We could avoid strong secondary effects of depletion and integrate physiological studies with molecular analyses because of the availability of a sequenced genome. The analyses presented in this paper indicate that Cu depletion affects the major Cu proteins, PC, Cu/ZnSOD, and PPO, especially in the younger leaves. Interestingly, the abundance of COXII, which is a core subunit of the mitochondrial Cu enzyme COX, was not affected, at least under the conditions that we studied. This remarkable observation suggests that Cu delivery to the mitochondria is a very high priority, which under deficiency supersedes delivery to the chloroplasts. Importantly, when Cu is resupplied, it is very quickly allocated to PC, especially in the younger leaves, with an immediate recovery of photosynthetic electron transport activity. Remarkably, PC content recovers much faster than PPO and Cu/ZnSOD activity. The recovery of PC and photosynthetic activity in young leaves even outpaces that of Cu/ZnSOD in the stem, an organ through which Cu must pass to reach the developing leaves at the top of the stem. Together, these observations provide solid support for a Cu economy model in which the priorities are first the mitochondrial and second the chloroplastic electron transport activities, which together are the plant cell's key "power generators."

In *Chlamydomonas*, genetic evidence has suggested that PC is actively degraded by a protease activity

Figure 7. Effects of Cu resupply to Cu-starved plants on the abundance and activity of Cu proteins. Poplar cuttings were grown hydroponically without added Cu as described in Figure 1. After 5 weeks, 50 nM Cu was added to the medium of plants previously grown in the absence of Cu. Plants continuously grown with 50 nM CuSO$_4$ (+) or without added Cu (−) were used as controls. Immunoblots for PC (PCa/b), the cytosolic (CSD1a/b) and the plastidial (CSD2a/b) Cu/ZnSODs, and the loading control (cFBPase; A and B) and in-gel SOD and PPO activity assays (C and D) are presented for developing leaves (A and C) and mature leaves (B and D). Experiments were conducted as already described in Figures 3, 4, and 6.

Figure 8. Cu-deficient poplar preferentially allocates available Cu to PC in the developing leaves. Poplar cuttings were grown hydroponically as described in Figure 1. After 5 weeks, 50 nM CuSO$_4$ was added to the medium of plants previously grown in the absence of Cu. Plants continuously grown in the presence or absence of Cu were used as controls. Protein and activity levels before (0) and 1, 2, 3, and 5 d after Cu addition were calculated relative to the value obtained for the Cu-sufficient plants and are presented as percentages. A, Cu content recovery in developing and mature leaves. Cu content was measured by ICP-AES. Values are given as averages ± SD (n = 4). B and C, Recovery of PC (PCa/b) and Cu/ZnSOD (CSD1a/b and CSD2a/b) protein abundance in developing (B) and mature (C) leaves. Immunoblotting was conducted as described in the legends of Figures 3 and 4. D and E, Recovery of Cu/ZnSOD activity, PPO activity, and ETR in developing (D) and mature (E) leaves. In-gel SOD and PPO activity assays and ETR measurements were conducted as described in Figures 4A, 6A, and 2A, respectively. For quantification of the gels/membranes, signal intensities were analyzed using ImageJ software, and quantitative regression curves were obtained using dilution series on the corresponding gel/membrane. Values are given as averages ± SD.
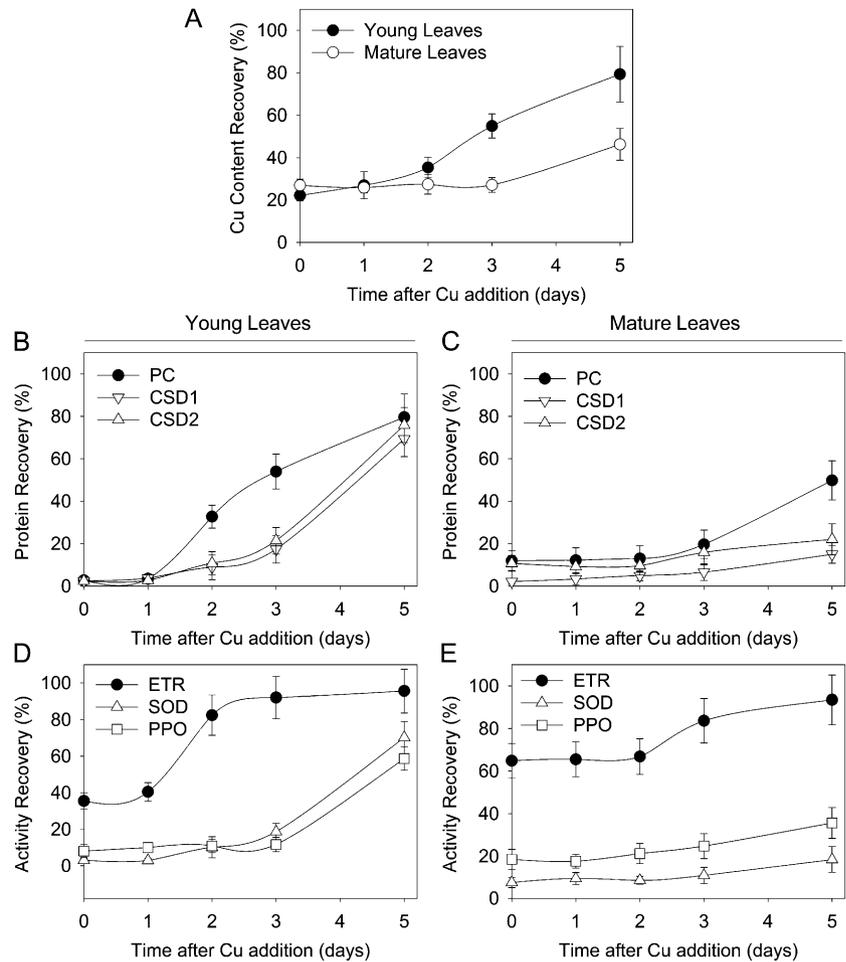
upon Cu depletion (Li and Merchant, 1995). This might facilitate the redistribution of Cu in *Chlamydomonas* that also expresses a cytochrome c_6, which can functionally replace PC (Merchant et al., 2006). However, in plants, which do not have a functional cytochrome c_6 (Molina-Heredia et al., 2003) and where PC is essential (Weigel et al., 2003), there is no experimental evidence for the induction of PC-specific proteolytic activity. It seems likely that apoPC without its cofactor is more rapidly turned over (see discussion in Abdel-Ghany, 2009). It had been suggested based on biophysical studies with isolated PC proteins that the two poplar PC isoforms differed in their thermal stability (Shosheva et al., 2005), and such differences might affect how tight the proteins bind a cofactor, which, in turn, could affect the stability of the polypeptide. The two poplar PC isoforms have very similar mobility on SDS-PAGE and therefore are not as easily distinguished as the Arabidopsis PC1 and PC2 isoforms (Pesaresi et al., 2009). Nevertheless, virtually all PC was lost upon Cu deficiency, which indicates that both poplar PC isoforms were equally affected in the end in vivo. In contrast, it had been observed for Arabidopsis that only the more abundant PC2 isoform was affected by low Cu (Abdel-Ghany, 2009). How-

ever, the study by Abdel-Ghany (2009) did not induce very severe deficiency, in which case both PC isoforms may suffer.

In miRBase (http://www.mirbase.org/search.shtml), there are no miRNAs listed that could target PC transcripts, and low Cu deficiency only had a moderate effect on PC transcripts, especially in young leaves. Therefore, we ascribe most of the loss of PC abundance and activity to lack of the cofactor. What could cause the reduced PC mRNA levels on low Cu in young leaves in the absence of a miRNA target site? Younger leaves were already becoming chlorotic after 5 weeks of depletion, indicating the onset of secondary effects. PC expression requires green photosynthetically active plastids, and it has been shown that the Arabidopsis *PC1* promoter contains a cis-acting region that mediates this response (Vorst et al., 1993). The reduction of PC mRNA levels in young Cu-depleted leaves, therefore, is most likely caused by early secondary effects as an indirect consequence of Cu depletion.

In contrast, the decrease in CSD and PPO activities on low Cu could be fully explained by the drastic reduction in the corresponding transcripts. The decreased abundance of these transcripts is correlated with the up-regulation of the Cu miRNAs *miR398* and

miR1444, which in their promoter areas are enriched in *GTAC* putative Cu-responsive elements for recognition by the SPL7 homolog of poplar. Two other conserved Cu miRNAs, *miR397* and *miR408*, target laccases in Arabidopsis (Sunkar and Zhu, 2004; Abdel-Ghany and Pilon, 2008). In poplar, three loci encode for *miR397* and one for *miR408*. The region of 500 bp upstream of the stem loop for all these miRNA loci is also enriched with multiple putative Cu-regulatory elements (Supplemental Fig. S2). As expected, these miRNAs were also up-regulated in poplar when Cu was depleted (Supplemental Fig. S7), which indicates that the miRNA- and SPL7-mediated responses to low Cu are indeed conserved in poplar.

In Arabidopsis, the major FeSOD gene, *FSD1*, is probably directly activated by SPL7 (Yamasaki et al., 2009), and FSD1 abundance is strongly induced when Cu is limited (Abdel-Ghany et al., 2005). However, we did not observe any FeSOD activity on low Cu in poplar (Supplemental Fig. S8). Indeed, database searches only yielded homologs of the Arabidopsis FeSOD isoforms *FSD2* and *FSD3*, whereas a homolog of *FSD1* seems to be absent from the poplar genome (data not shown). Therefore, induction of a major FeSOD counterpart, which is a signature of Cu limitation and deficiency in Arabidopsis, is not a response in poplar (Supplemental Fig. S8). Previously, the induction of FeSOD activity was also not observed in maize (Cohu and Pilon, 2007). Therefore, FSD1 induction as a backup for CSD2 should not be considered as a general response to Cu deficiency in higher plants.

The protein band identified as PPO12 was highly abundant on Coomassie Brilliant Blue-stained SDS-PAGE gels (Fig. 4). Activity gels indicate that several PPOs are active (Fig. 5). Therefore, PPO constitutes a major sink for Cu in the thylakoids in poplar but is absent from Arabidopsis. The miRNA *miR1444* targets all plastid PPOs. All three *miR1444* loci are enriched in *GTAC* motifs in their promoter areas, and they are up-regulated when Cu becomes limiting. Therefore, *miR1444* is a new Cu miRNA. Since PPO and PC are active within the same thylakoid lumen compartment, they would be expected to compete for Cu directly. In this regard, the down-regulation of PPO on limited Cu would make sense if plants benefit from targeting the remaining Cu to PC. The faster recovery or ETR activity compared with PPO activity when Cu is resupplied indicates that this adaptation seems to work.

The biological role of PPO is not yet fully understood, but induction of PPO by wounding in *P. trichocarpa* (Fig. 6) and in hybrid poplar (Constabel et al., 2000) suggests that it is involved in biotic responses. During herbivory, the cell membranes are disrupted, which would allow the thylakoid-localized PPOs to gain access to phenolic substrates sequestered in other cellular compartments to generate chemicals that deter or inhibit the herbivore. Therefore, following wounding, PPO should have preferential access to Cu, bypassing the "regular" priority pathway to PC. Both PC and PPO are nucleus encoded and have

bipartite targeting signals composed of a chloroplast transit peptide to reach the stroma and a signal peptide for the thylakoid lumen. PC reaches the thylakoid lumen via the Sec pathway, which takes unfolded proteins (for review, see Jarvis, 2008). Therefore PC gets its Cu cofactor in the lumen, where Cu is delivered by PAA2. However, the PPO signal sequence has a twin Arg motif and therefore should follow the TAT pathway for thylakoid transfer, which allows folded proteins to be transported. Therefore, PPO could acquire its cofactor in the stroma, where it would not compete with PC for available luminal Cu. Thus, PPO might become a priority target for Cu delivery in the chloroplast upon induction by wounding as long as sufficient Cu is available. On the other hand, sustained cofactor delivery of PC during Cu depletion would require the down-regulation of PPO, which is achieved by *miR1444* up-regulation. The simultaneous down-regulation of *CCS* and *CSD2*, which are both targets of *miR398*, would lead to the elimination of all competing Cu sinks in the chloroplast. As a consequence in depleted plants, any Cu that becomes available can be prioritized to PC, which is apparently the preferred target (Fig. 8). Other major Cu proteins, such as chloroplastic PPOs and CSD2, as well as cytosolic CSD1 and the secreted laccases, which are targets of the conserved *miR397* and *miR408* (Abdel-Ghany and Pilon, 2008), are apparently dispensable when Cu is limiting.

Surprisingly, we observed increases in contents for Mn and Zn for Cu-depleted plants, especially in mature leaves (Supplemental Table S1). The increases in Mn and Zn without changes in Fe contents are reminiscent of the Fe deficiency-induced changes observed in shoots of soil-grown Arabidopsis, where also cadmium and cobalt were increased (Baxter et al., 2008). The nonessential elements cadmium and cobalt, however, were not present in our growth medium and therefore were not detected. The relatively healthy appearance of the plants and the rather modest changes in chlorophyll contents of the Cu-depleted poplars are not indicative of severe Fe deficiency symptoms (Marschner, 1995). Furthermore, we did not see a change in molybdenum contents (data not shown), a decrease of which was part of the reported signature of Fe deficiency in Arabidopsis (Baxter et al., 2008). The changes in Mn and Zn content in poplar leaves in response to Cu depletion, therefore, remain to be explained.

Trace elements such as Fe, Mn, molybdenum, nickel, Zn, and Cu are required to form cofactors of enzymes. Early studies in hydroponic systems defined the nutritional requirements of plants and indicated the physiological consequences of deficiencies (Arnon and Stout, 1939). Follow-up studies helped to identify biochemical functions of specific metalloenzymes (Marschner, 1995). In the case of Cu, however, the remarkable status of the field is that the biological significance of Cu proteins other than PC, COX, and the ethylene receptors remains elusive even though the vast majority of the Cu-requiring

enzymatic activities have been identified (for review, see Burkhead et al., 2009; Cohu and Pilon, 2010). The use of forward and reverse genetics in the genomic era mainly in Arabidopsis has allowed the identification of metal transporters, assembly factors, and transcriptional regulators; now, at least in the case of Cu, most but certainly not all factors seem to be identified (Burkhead et al., 2009). Nutritional homeostasis in a changing environment requires the concerted and coordinated action of transporters and sensors together with the tuning of the expression of metal cofactor-requiring enzymes. A complete understanding of metal homeostasis requires a model that allows a spatiotemporal analysis of plant responses to varying nutrient supply under conditions where secondary effects of deficiency and toxicity are minimal and where physiological studies can be integrated with molecular level data. This study highlights the suitability of poplar grown in hydroponics as a model in the postgenomic era for studies of nutritional homeostasis, as it allowed us to establish clear priorities in Cu delivery during deficiency and recovery. Future studies on this model should employ reverse genetics to highlight the kinetic roles of individual Cu homeostasis factors, and this approach also has great promise to reveal novel biological roles of Cu enzymes.

MATERIALS AND METHODS

Plant Material and Growth Conditions

Clones of poplar (*Populus trichocarpa* Nisqually-1) were propagated in a greenhouse from greenwood cuttings collected from 3- to 6-month-old trees grown in soil (Pro Mix BX Mycorise Pro; Premier Horticulture). To start hydroponic culture, we used 8-cm-tall apical stem cuttings (one per branch). Cuttings originating from the same plant were randomly distributed over treatments. Cuttings were rooted using an indole butyric acid-containing mixture (Clonex; Hydrodynamics International) and kept in vermiculite under saturated humidity. After rooting (approximately 1 week), the clones were transplanted into 20-L plastic buckets (six plants per bucket) containing one-tenth-strength modified Hoagland solution (Epstein and Bloom, 2005). The nutrient solution was aerated and replaced weekly. For growth under Cu depletion, Cu was omitted from the medium, while 50 nM $CuSO_4$ was added for the Cu-sufficient condition. To minimize Cu contamination, deionized water was used from rooting to hydroponic growth. All plants were grown in a growth chamber under a light intensity of 100 μmol m^{-2} s^{-1}, with a 16-h-light/8-h-dark cycle and temperature maintained at 21°C ± 1°C.

Plant Sampling

All experiments were performed with at least three biological replicates. Leaves were numbered using the LPI system (Larson and Isebrands, 1971), with the index leaf (LPI 0) defined as the first developing leaf of more than 2 cm. Sampling was partitioned into young leaves (LPI 0–2), mature leaves (LPI 3–9), stem, and roots. Material from two to three plants was pooled into a single sample, immediately frozen in liquid nitrogen, and stored frozen until further analysis. For wounding treatments, leaves (LPI 3–9) were perforated with a hole puncher (diameter of 7 mm) once and leaf tissue (LPI 0–9) was collected after 2 d. For chlorophyll fluorescence measurements, leaves LPI 2 and 5 were studied as young leaves and mature leaves, respectively.

Elemental Analysis

To remove residual nutrient solution, root samples were washed for 10 min in dideionized water, then for 20 min in 40 mM EDTA, and again rinsed for 10 min in dideionized water. One gram (fresh weight) of young leaves, mature leaves, stem, and roots was dried for 1 week at 55°C. Depending on the sample analyzed, 50 to 200 mg of dried tissue was digested in 1 mL of nitric acid and heated for 2 h at 60°C and for 6 h at 130°C. Resulting digests were diluted up to 10 mL with dideionized water and analyzed using inductively coupled plasma-atomic emission spectrometry (ICP-AES) as described by Pilon-Smits et al. (1999).

Protein Accumulation and Enzyme Activity

Soluble proteins for nondenaturing and SDS-polyacrylamide gel analysis were extracted as described (Abdel-Ghany et al., 2005). Protein concentration was determined according to Bradford (1976) using bovine serum albumin as a standard. Each experiment was done at least in biological triplicate with identical results, and representative gels are shown. Quantification of the signals was performed using calibration curves based on dilution series of control plus Cu-grown plant samples. Signal intensity was determined using ImageJ software, and regression curves were determined using SigmaPlot software (version 7.4; Systat Software). Quantitative data are means of two dilution series analyses. To estimate protein molecular masses, the BenchMark Prestained Protein Ladder (Invitrogen) was used.

Antibodies used for immunodetection of CSD1, PC, and CSD2 have been described (Kliebenstein et al., 1998; Abdel-Ghany et al., 2005; Cohu et al., 2009). cFBPase and COXII antibodies were purchased from AgriSera and used at recommended dilutions. For western blotting, 20 μg of total protein was separated by 15% SDS-PAGE and then transferred onto a nitrocellulose membrane.

For in-gel SOD activity analysis, 40 μg of native protein extract was fractionated on a 15% nondenaturing gel and then stained for activity as described (Beauchamp and Fridovich, 1971). For in-gel PPO activity, 20 μg of native protein extract was fractionated on a 10% SDS-PAGE gel and tested for PPO activity using the dihydroxy-Phe assay as described previously by Constabel et al. (2000). To measure PPO-mediated browning, leaf tissue was ground in 100 mM citrate phosphate buffer (pH 6.0) essentially as described by Wang and Constabel (2004). Briefly, native protein extract (400 μg) was diluted in 1 mL of 100 mM citrate phosphate buffer (pH 6.0) and incubated for 36 h at room temperature. Tropolone, a specific PPO inhibitor, was used at a final concentration of 400 μM in control samples.

Proteomic Analysis

For protein identification, 100 μg of total leaf protein was separated on a large (20 × 15 cm) Coomassie Brilliant Blue-stained 15% SDS-PAGE gel. The gel band was excised and subjected to trypsin digestion. The sample was subsequently analyzed using an online reverse-phase capillary flow HPLC device coupled to an electrospray ionization source on the LTQ linear ion trap mass spectrometer at the Colorado State University proteomics facility. The SEQUEST search engine was used to search the acquired tandem mass spectrometry spectra, and the resulting protein identifications were further validated using Scaffold proteomics software (Proteome Software). For each band, two digestion pattern analyses were performed.

Chlorophyll Fluorescence Measurements

Chlorophyll fluorescence was measured with an FMS2 Fluorometer (Hansatech Instruments) essentially as described previously by Cohu and Pilon (2007). The light-adapted parameters were determined at actinic light intensities of 40, 100, 300, 600, 900, and 1,500 μmol m^{-2} s^{-1}. Plants were dark adapted for 1 h prior to analysis. All parameters were calculated according to Maxwell and Johnson (2000).

Sequence Retrieval and Analysis

To retrieve poplar protein sequences, a BLAST of Arabidopsis (*Arabidopsis thaliana*) amino acid sequences (http://www.arabidopsis.org) was performed on the poplar genome (taxid:3694) using the Entrez protein database available at the National Center for Biotechnology Information (NCBI; http://ncbi.nlm.nih.gov). The multiple sequence alignments and the phylogenic relationships among amino acid sequences were determined using ClustalW (http://www.genome.jp/tools/clustalw), using the default settings. Subcellular localization was predicted using TargetP (http://www.cbs.dtu.dk/services/TargetP). Potential miRNA target sites among nucleic acid sequences were identified using miRBase (http://www.mirbase.org/search.shtlm), using e = 100 as a cutoff.

Quantitative Reverse Transcription-PCR

Total RNA was extracted using Trizol reagent (Invitrogen) according to the manufacturer's recommendations. cDNA synthesis, quality control, and quantitative reverse transcription (qRT)-PCR were performed in a Roche Light Cycler 480 according to the method described by Girin et al. (2007). PCR amplification of the various genes analyzed was performed using the gene-specific primers listed in Supplemental Table S2. The *PCa* transcript harbors a 3′ untranslated region not found in *PCb*; therefore, it could be detected separately. Due to sequence similarity, *PCb* could only be detected with a primer pair that also amplifies PCa. Due to high similarity *PPO2, -4, -5,* and *-9* were also amplified with a single primer pair. The qRT-PCR results were analyzed using Light-Cycler 480 data-analysis software. Relative transcript levels ($2^{-\Delta Ct}$) were evaluated by calculation of the difference between the cycle threshold value of the target gene (Ct target) and the cycle threshold value of the control gene (Ct reference) for the respective templates (Arrivault et al., 2006). Gene expression was monitored in technical duplicate and biological triplicate, and the results were standardized using Actin1. Similar results were obtained using EF1α as a reference (data not shown).

Mature miRNA Stem-Loop qRT-PCR

For the stem-loop pulsed RT, total RNA was extracted using Trizol reagent (Invitrogen) according to the manufacturer's recommendations. However, ethanol washes were avoided and nucleic acid precipitation steps were performed using 1:1 (v/v) isopropanol and 1:10 (v/v) sodium acetate (3 M; pH 5.2) in order to optimize small RNA molecule retrieval. The stem-loop pulsed RT and miRNA qRT-PCR were performed as described previously (Varkonyi-Gasic and Hellens, 2007) using the primers listed in Supplemental Table S2. Analysis of the data was performed as described above. Mature miRNA abundance was monitored in biological triplicate with a technical duplicate for each sample, and the results were standardized using *miR156* expression. Similar results were obtained using *miR472* as a reference (data not shown).

Statistical Analysis

JMP software (version 9.0.2; SAS Institute) was used for statistical analysis. Figures and data represent average and SD values based on sampling from at least three independent biological replicates. The number of total samples (*n*) is given when appropriate. Student's *t* test was used to calculate significant differences ($P < 0.05$), which is reported in the text or figures where appropriate.

Sequence data from this article can be found in the GenBank/EMBL data libraries under the accession numbers provided in Table I.

Supplemental Data

The following materials are available in the online version of this article.

Supplemental Figure S1. In silico analysis of the CCS/CSD family in poplar.

Supplemental Figure S2. The poplar Cu miRNAs present potential Cu-responsive elements in their promoter.

Supplemental Figure S3. Proteomic identification of PPO12.

Supplemental Figure S4. In silico analysis of the PPO family in poplar.

Supplemental Figure S5. Effects of Cu deficiency on COXII abundance.

Supplemental Figure S6. Effects of Cu resupply on the abundance and activity of Cu proteins in poplar stem and roots.

Supplemental Figure S7. *miR397* and *miR408* are regulated by Cu in poplar.

Supplemental Figure S8. An FeSOD is not detected in poplar leaves.

Supplemental Table S1. Effects of Cu deficiency on mineral content.

Supplemental Table S2. List of the primers used for qRT-PCR and mature miRNA stem-loop qRT-PCR.

ACKNOWLEDGMENTS

LITERATURE CITED

Abdel-Ghany SE (2009) Contribution of plastocyanin isoforms to photosynthesis and copper homeostasis in *Arabidopsis thaliana* grown at different copper regimes. Planta **229:** 767–779

Abdel-Ghany SE, Müller-Moulé P, Niyogi KK, Pilon M, Shikanai T (2005) Two P-type ATPases are required for copper delivery in *Arabidopsis thaliana* chloroplasts. Plant Cell **17:** 1233–1251

Abdel-Ghany SE, Pilon M (2008) MicroRNA-mediated systemic downregulation of copper protein expression in response to low copper availability in Arabidopsis. J Biol Chem **283:** 15932–15945

Andrés-Colás N, Perea-García A, Puig S, Peñarrubia L (2010) Deregulated copper transport affects Arabidopsis development especially in the absence of environmental cycles. Plant Physiol **153:** 170–184

Andrés-Colás N, Sancenón V, Rodríguez-Navarro S, Mayo S, Thiele DJ, Ecker JR, Puig S, Peñarrubia L (2006) The Arabidopsis heavy metal P-type ATPase HMA5 interacts with metallochaperones and functions in copper detoxification of roots. Plant J **45:** 225–236

Arnon DI, Stout PR (1939) The essentiality of certain elements in minute quantity for plants with special reference to copper. Plant Physiol **14:** 371–375

Arrivault S, Senger T, Krämer U (2006) The Arabidopsis metal tolerance protein AtMTP3 maintains metal homeostasis by mediating Zn exclusion from the shoot under Fe deficiency and Zn oversupply. Plant J **46:** 861–879

Baxter IR, Vitek O, Lahner B, Muthukumar B, Borghi M, Morrissey J, Guerinot ML, Salt DE (2008) The leaf ionome as a multivariable system to detect a plant's physiological status. Proc Natl Acad Sci USA **105:** 12081–12086

Beauchamp C, Fridovich I (1971) Superoxide dismutase: improved assays and an assay applicable to acrylamide gels. Anal Biochem **44:** 276–287

Bernal M, Testillano PS, Alfonso M, del Carmen Risueño M, Picorel R, Yruela I (2007) Identification and subcellular localization of the soybean copper P1B-ATPase GmHMA8 transporter. J Struct Biol **158:** 46–58

Bradford MM (1976) A rapid and sensitive method for the quantitation of microgram quantities of protein utilizing the principle of protein-dye binding. Anal Biochem **72:** 248–254

Burkhead JL, Reynolds KA, Abdel-Ghany SE, Cohu CM, Pilon M (2009) Copper homeostasis. New Phytol **182:** 799–816

Carr HS, Winge DR (2003) Assembly of cytochrome c oxidase within the mitochondrion. Acc Chem Res **36:** 309–316

Chu CC, Lee WC, Guo WY, Pan SM, Chen LJ, Li HM, Jinn TL (2005) A copper chaperone for superoxide dismutase that confers three types of copper/zinc superoxide dismutase activity in Arabidopsis. Plant Physiol **139:** 425–436

Cohu CM, Abdel-Ghany SE, Gogolin Reynolds KA, Onofrio AM, Bodecker JR, Kimbrel JA, Niyogi KK, Pilon M (2009) Copper delivery by the copper chaperone for chloroplast and cytosolic copper/zinc-superoxide dismutases: regulation and unexpected phenotypes in an Arabidopsis mutant. Mol Plant **2:** 1336–1350

Cohu CM, Pilon M (2007) Regulation of superoxide dismutase expression by copper availability. Physiol Plant **129:** 747–755

Cohu CM, Pilon M (2010) Cell biology of copper. *In* R Hell, RR Mendel, eds, Plant Cell Monographs: Cell Biology of Metals and Nutrients, Vol 17. Springer, Heidelberg, pp 55–74

Constabel CP, Yip L, Patton JJ, Christopher ME (2000) Polyphenol oxidase from hybrid poplar: cloning and expression in response to wounding and herbivory. Plant Physiol **124:** 285–295

Dugas DV, Bartel B (2008) Sucrose induction of Arabidopsis miR398 represses two Cu/Zn superoxide dismutases. Plant Mol Biol **67:** 403–417

Epstein E, Bloom AJ (2005) Mineral Nutrition of Plants: Principles and Perspectives. Ed 2. Sinauer Associates, Sunderland, MA, pp 17–39

Garcia-Molina A, Andrés-Colás N, Perea-García A, Del Valle-Tascón S, Peñarrubia L, Puig S (2011) The intracellular Arabidopsis COPT5 transport protein is required for photosynthetic electron transport under severe copper deficiency. Plant J **65:** 848–860

Girin T, Lejay L, Wirth J, Widiez T, Palenchar PM, Nazoa P, Touraine B, Gojon A, Lepetit M (2007) Identification of a 150 bp cis-acting element of the AtNRT2.1 promoter involved in the regulation of gene expression by the N and C status of the plant. Plant Cell Environ **30:** 1366–1380

Ravet et al.

Hoagland DR, Arnon DI (1950) The water culture method for growing plants without soil. Calif Agric Exp Sta Circ 347

Hirayama T, Kieber JJ, Hirayama N, Kogan M, Guzman P, Nourizadeh S, Alonso JM, Dailey WP, Dancis A, Ecker JR (1999) RESPONSIVE-TO-ANTAGONIST1, a Menkes/Wilson disease-related copper transporter, is required for ethylene signaling in Arabidopsis. Cell 97: 383–393

Jarvis P (2008) Targeting of nucleus-encoded proteins to chloroplasts in plants. New Phytol 179: 257–285

Kahn V, Andrawis A (1985) Inhibition of mushroom tyrosinase by tropolone. Phytochemistry 25: 905–908

Kampfenkel K, Kushnir S, Babiychuk E, Inzé D, Van Montagu M (1995) Molecular characterization of a putative Arabidopsis thaliana copper transporter and its yeast homologue. J Biol Chem 270: 28479–28486

Kliebenstein DJ, Monde RA, Last RL (1998) Superoxide dismutase in Arabidopsis: an eclectic enzyme family with disparate regulation and protein localization. Plant Physiol 118: 637–650

Kropat J, Tottey S, Birkenbihl RP, Depege N, Huijser P, Merchant S (2005) A regulator of nutritional copper signaling in Chlamydomonas is an SBP domain protein that recognizes the GTAC core of copper response element. Proc Natl Acad Sci USA 102: 18730–18735

Larson PR, Isebrands JG (1971) The plastochron index as applied to developmental studies of cottonwood. Can J Res 1: 1–11

Li HH, Merchant SS (1995) Degradation of plastocyanin in copper-deficient Chlamydomonas reinhardtii: evidence for a protease-susceptible conformation of the apoprotein and regulated proteolysis. J Biol Chem 270: 23504–23510

Lu S, Sun YH, Chiang VL (2008) Stress-responsive microRNAs in Populus. Plant J 55: 131–151

Marschner H (1995). Mineral Nutrition of Higher Plants. Academic Press, London

Maxwell K, Johnson GN (2000) Chlorophyll fluorescence: a practical guide. J Exp Bot 51: 659–668

Mayer AM (2006) Polyphenol oxidases in plants and fungi: going places? A review. Phytochemistry 67: 2318–2331

Merchant SS, Allen MD, Kropat J, Moseley JL, Long JC, Tottey S, Terauchi AM (2006) Between a rock and a hard place: trace element nutrition in Chlamydomonas. Biochim Biophys Acta 1763: 578–594

Molina-Heredia FP, Wastl J, Navarro JA, Bendall DS, Hervás M, Howe CJ, De La Rosa MA (2003) Photosynthesis: a new function for an old cytochrome? Nature 424: 33–34

Müller P, Li XP, Niyogi KK (2001) Non-photochemical quenching: a response to excess light energy. Plant Physiol 125: 1558–1566

Pesaresi P, Scharfenberg M, Weigel M, Granlund I, Schröder WP, Finazzi G, Rappaport F, Masiero S, Furini A, Jahns P, et al (2009) Mutants, overexpressors, and interactors of Arabidopsis plastocyanin isoforms: revised roles of plastocyanin in photosynthetic electron flow and thylakoid redox state. Mol Plant 2: 236–248

Pilon M, Ravet K, Tapken W (2011) The biogenesis and physiological function of chloroplast superoxide dismutases. Biochim Biophys Acta 1807: 989–998

Pilon-Smits EA, Hwang S, Mel Lytle C, Zhu Y, Tai JC, Bravo RC, Chen Y, Leustek T, Terry N, (1999) Overexpression of ATP sulfurylase in Indian mustard leads to increased selenate uptake, reduction, and tolerance. Plant Physiol 119: 123–132

Puig S, Andrés-Colás N, García-Molina A, Peñarrubia L (2007) Copper and iron homeostasis in Arabidopsis: responses to metal deficiencies, interactions and biotechnological applications. Plant Cell Environ 30: 271–290

Puig S, Peñarrubia L (2009) Placing metal micronutrients in context: transport and distribution in plants. Curr Opin Plant Biol 12: 299–306

Raven JA, Ewans CWE, Korb RE (1999) The role of trace metals in photosynthetic electron transport in O_2-evolving organisms. Photosynth Res 60: 111–149

Rodríguez FI, Esch JJ, Hall AE, Binder BM, Schaller GE, Bleecker AB (1999) A copper cofactor for the ethylene receptor ETR1 from Arabidopsis. Science 283: 996–998

Sancenón V, Puig S, Mateu-Andrés I, Dorcey E, Thiele DJ, Peñarrubia L (2004) The Arabidopsis copper transporter COPT1 functions in root elongation and pollen development. J Biol Chem 279: 15348–15355

Sancenón V, Puig S, Mira H, Thiele DJ, Peñarrubia L (2003) Identification of a copper transporter family in Arabidopsis thaliana. Plant Mol Biol 51: 577–587

Schubert M, Petersson UA, Haas BJ, Funk C, Schröder WP, Kieselbach T (2002) Proteome map of the chloroplast lumen of Arabidopsis thaliana. J Biol Chem 277: 8354–8365

Shikanai T, Müller-Moulé P, Munekage Y, Niyogi KK, Pilon M (2003) PAA1, a P-type ATPase of Arabidopsis, functions in copper transport in chloroplasts. Plant Cell 15: 1333–1346

Shosheva A, Donchev A, Dimitrov M, Kostov G, Toromanov G, Getov V, Alexov E (2005) Comparative study of the stability of poplar plastocyanin isoforms. Biochim Biophys Acta 1748: 116–127

Sunkar R, Kapoor A, Zhu JK (2006) Posttranscriptional induction of two Cu/Zn superoxide dismutase genes in Arabidopsis is mediated by downregulation of miR398 and important for oxidative stress tolerance. Plant Cell 18: 2051–2065

Sunkar R, Zhu JK (2004) Novel and stress-regulated microRNAs and other small RNAs from Arabidopsis. Plant Cell 16: 2001–2019

Tabata K, Kashiwagi S, Mori H, Ueguchi C, Mizuno T (1997) Cloning of a cDNA encoding a putative metal-transporting P-type ATPase from Arabidopsis thaliana. Biochim Biophys Acta 1326: 1–6

Tuskan GA, Difazio S, Jansson S, Bohlmann J, Grigoriev I, Hellsten U, Putnam N, Ralph S, Rombauts S, Salamov A, et al (2006) The genome of black cottonwood, Populus trichocarpa (Torr. & Gray). Science 313: 1596–1604

Valero E, Garcia-Moreno M, Varon R, Garcia-Carmona F (1991) Time-dependent inhibition of grape polyphenol oxidase by tropolone. J Agric Food Chem 39: 1043–1046

Varkonyi-Gasic E, Hellens RP (2007) Quantitative stem-loop RT-PCR for detection of microRNAs. Methods Mol Biol 744: 145–157

Vorst O, Kock P, Lever A, Weterings B, Weisbeek P, Smeekens S (1993) The promoter of the Arabidopsis thaliana plastocyanin gene contains a far upstream enhancer-like element involved in chloroplast-dependent expression. Plant J 4: 933–945

Wang J, Constabel CP (2004) Polyphenol oxidase overexpression in transgenic Populus enhances resistance to herbivory by forest tent caterpillar (Malacosoma disstria). Planta 220: 87–96

Waters BM, Grusak MA (2008) Whole-plant mineral partitioning throughout the life cycle in Arabidopsis thaliana ecotypes Columbia, Landsberg erecta, Cape Verde Islands, and the mutant line ysl1ysl3. New Phytol 177: 389–405

Weigel M, Varotto C, Pesaresi P, Finazzi G, Rappaport F, Salamini F, Leister D (2003) Plastocyanin is indispensable for photosynthetic electron flow in Arabidopsis thaliana. J Biol Chem 278: 31286–31289

Yamasaki H, Abdel-Ghany SE, Cohu CM, Kobayashi Y, Shikanai T, Pilon M (2007) Regulation of copper homeostasis by micro-RNA in Arabidopsis. J Biol Chem 282: 16369–16378

Yamasaki H, Hayashi M, Fukazawa M, Kobayashi Y, Shikanai T (2009) SQUAMOSA promoter binding Protein-Like7 is a central regulator for copper homeostasis in Arabidopsis. Plant Cell 21: 347–361